

Characterization of electron microscopes with binary pseudo-random multilayer test samples

Valeriy V. Yashchuk^{a,*}, Raymond Conley^b, Erik H. Anderson^c, Samuel K. Barber^a,
Nathalie Bouet^b, Wayne R. McKinney^a, Peter Z. Takacs^d, Dmitriy L. Voronov^a

^aAdvanced Light Source, Lawrence Berkeley National Laboratory, Berkeley, CA 94720, USA

^bNSLS-II, Brookhaven National Laboratory, Upton, NY 11973, USA

^cCenter for X-ray Optics, Lawrence Berkeley National Laboratory, Berkeley, CA 94720, USA

^dBrookhaven National Laboratory, Upton, NY 11973, USA

* E-mail: vvyashchuk@lbl.gov; Phone: +1-510-495-2592; Fax: +1-510-486-7696

ABSTRACT

Verification of the reliability of metrology data from high quality x-ray optics requires that adequate methods for test and calibration of the instruments be developed. For such verification for optical surface profilometers in the spatial frequency domain, a modulation transfer function (MTF) calibration method based on binary pseudo-random (BPR) gratings and arrays has been suggested [Proc. SPIE 7077-7 (2007), Opt. Eng. 47(7), 073602-1-5 (2008)] and proven to be an effective calibration method for a number of interferometric microscopes, a phase shifting Fizeau interferometer, and a scatterometer [Nucl. Instr. and Meth. A 616, 172-82 (2010)]. Here we describe the details of development of binary pseudo-random multilayer (BPRML) test samples suitable for characterization of scanning (SEM) and transmission (TEM) electron microscopes. We discuss the results of TEM measurements with the BPRML test samples fabricated from a WiSi_2/Si multilayer coating with pseudo randomly distributed layers. In particular, we demonstrate that significant information about the metrological reliability of the TEM measurements can be extracted even when the fundamental frequency of the BPRML sample is smaller than the Nyquist frequency of the measurements. The measurements demonstrate a number of problems related to the interpretation of the SEM and TEM data. Note that similar BPRML test samples can be used to characterize x-ray microscopes. Corresponding work with x-ray microscopes is in progress.

Keywords: surface metrology, surface profilometer, interferometric microscope, modulation transfer function, power spectral density, calibration, error reduction, fabrication tolerances, metrology of x-ray optics

1. Introduction

Verification of the reliability of metrology data from high quality x-ray optics requires that adequate methods for test and calibration of the instruments be developed. For such verification for optical surface profilometers in the spatial frequency domain, a modulation transfer function (MTF) calibration method based on binary pseudo-random (BPR) gratings and arrays has been suggested [1,2] and proven to be an effective calibration method for a number of interferometric microscopes, a phase shifting Fizeau interferometer, and a scatterometer [3-6].

Unlike most conventional MTF test surfaces, the inherent power spectral density (PSD) of the BPR gratings and arrays has a deterministic white-noise-like character. This allows the direct determination of the one- (1D) and two-dimensional (2D) MTF, respectively, with a sensitivity uniform over the entire spatial frequency range of a profiler.

Here we describe binary pseudo-random multilayer (BPRML) test samples suitable for characterization of scanning (SEM) and transmission (TEM) electron microscopes. A BPRML sample is a multilayer structure consisting of two materials with significantly different contrasts when observed with an electron microscope, Fig. 1.

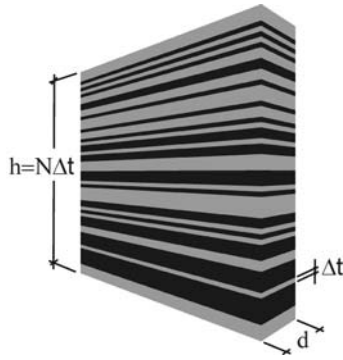


Figure 1: Structure of a BPR multilayer test pattern consisting of 63 elementary sub-layers of thickness Δt .

The thicknesses of the layers are distributed according to a binary pseudo-random sequence. For the MTF calibration of an electron microscope, an image of the BPR multilayer cross-section, measured with the microscope, is processed to get a power spectral density (PSD) distribution. The MTF is found as the square root of the ratio of the PSD spectrum measured with the BPRML to the ‘ideal’, spatial frequency independent, PSD spectrum, inherent for a precisely fabricated BPRML. We present and discuss PSD analysis on the lower magnification TEM images. The results of this analysis provide insight into how to interpret PSD analysis of the other TEM images.

2. Fabrication of BPR multilayer test samples

BPRML test samples suitable for measurements with scanning and transmission electron microscopes were made of a multilayer structure consisting of two materials, WSi_2 and Si that have significantly different contrasts when observed with an electron microscope. The multilayer consists of 1010 layers of the two materials with thicknesses pseudo-randomly distributed according to a binary pseudo-random sequence of $N=2047$ total elements [5]. The elementary thickness of the multilayer is $\Delta t = 3$ nm.

The SEM and TEM compatible samples were prepared from the multilayer with Dual Beam FIB (focused ion beam)/SEM processing. For the SEM measurements, the BPRML was cross-sectioned by FIB/SEM etching.

A test sample for measurements with a TEM was FIB etched out of the multilayer and attached to a pin of a standard TEM sample holder. It looks like a cross-section of a multilayer (Fig. 1) with thickness $\sim d=60$ -100 nm and overall size of approximately $10 \mu\text{m} \times 10 \mu\text{m}$. The details of the BPRML test sample fabrication can be found elsewhere [6].

3. PSD analysis of TEM measurements with the BPRML test sample

The previous study of binary pseudo random sequences and arrays [1-6] provides a good idea of what to expect from measurements of BPR samples with different relations between the sample’s fundamental size and the instrument’s pixel size. In the case of a BPRML measurement performed with a TEM at 17.5 keV electron energy, the pixel size of the instrument (~ 1 nm) is smaller than the fundamental layer thickness of the BPRML sample (3 nm) by a factor of about 3. Consequently, the BPRML sample is being sampled at a rate higher than the fundamental frequency of the sample. When the sequence is oversampled, there should be an oscillatory behavior that resembles a sinc squared function as shown in Fig. 2a. However, the PSD, calculated from the BPRML TEM image continues to decrease steeply instead of oscillating – Fig. 2b. Because of the apparent high quality of the images, this result is rather surprising. The spike seen in the measured PSDs occurring at around $350 \mu\text{m}^{-1}$ is a diffraction peak corresponding to the fundamental layer thickness. In fact, the actual layer thickness is about

2.8 nm and $f_0 \approx 179 \mu\text{m}^{-1}$, which almost exactly corresponds to the $350 \mu\text{m}^{-1}$ peak. A similar diffraction peak has been observed in the scatterometer measurements [5] of a BPR array with a fundamental size exceeded by 1.5 the wavelength of the scattered light.

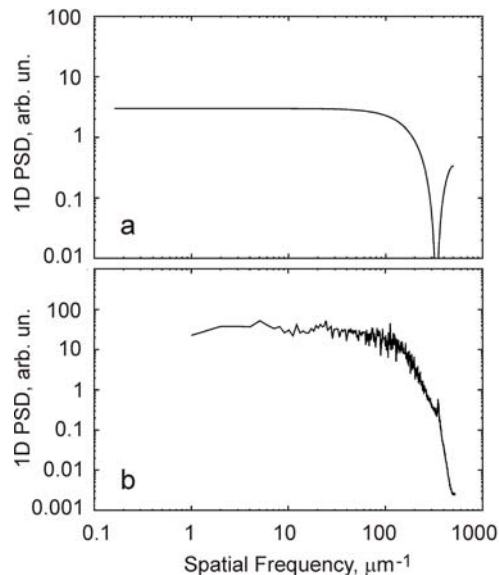


Figure 2: One-dimensional (1D) PSD of a binary pseudo random sequence with a fundamental element size of 3 nm sampled at rates of 3 nm (a) and 1 nm (b).

Note that the oscillatory spectral behavior related to oversampling is also an inherent property of the sequence (BPR grating) and has a deterministic character. This characteristic spectrum can be used as an ideal PSD of the sample when calibrating an instrument with resolution better than the fundamental size of the sample.

4. Probability distribution analysis of TEM images of the BPRML test sample

The impetus of this study is to understand why the PSDs in Fig. 2b of Ref. [2] obtained from an image shown in Fig. 3a, differ from the expected PSDs shown in Fig. 2a.

Figure 3b shows a plot of the intensity values across a single line of a single TEM image, Fig. 2a. There is a much tighter grouping of the low intensity values than of the high intensity values.

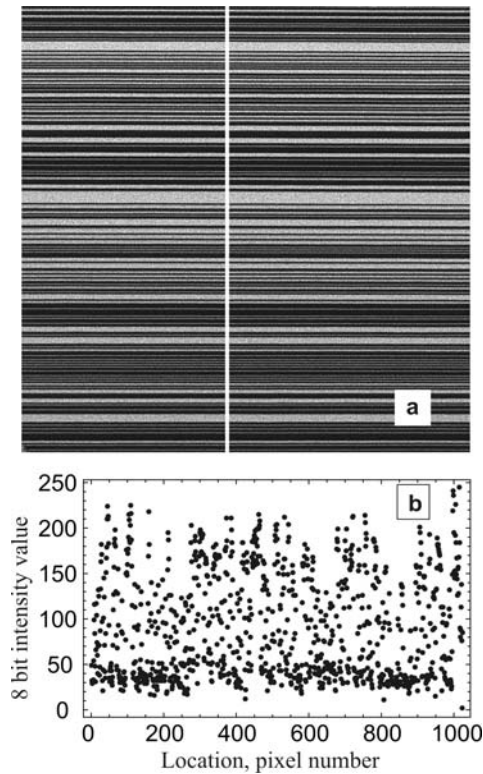


Figure 3: TEM image of BPRML sample (a) and plot of intensity values (b) along the red line in (a). Note the strong grouping of the low intensity values compared with high intensity values.

As we show below, the distortion to the TEM PSDs, discussed in Sec. 3, is related to the relatively large variation in the high intensity values compared with the variation of the low intensity values (Fig. 3b).

5. TEM image contrast and PSD spectra of the BPRML test sample

The problem was superficially treated by adjusting the image in Fig. 3a to sharpen it. This is accomplished by effectively reducing the intensity resolution in the high intensity regime. We define the high intensity regime to be intensity values greater than the value where the derivative of the image histogram is equal to zero between the two peaks, i.e. for Fig. 5 this value would be roughly 90. All intensity values in this regime are divided by 5 and rounded to the nearest integer. A constant offset is added to shift the reduced values back to the original range of the high intensity regime.

In spite of the crude procedure used for adjusting the TEM image contrast, the high frequency content in the PSD spectra from the adjusted image is significantly changed – Fig. 4 (compare with Fig. 2b). Instead of a steep decrease with increasing spatial frequency, we notice behavior that hints at the oscillations we expect to see, i.e. Fig. 2a. Also note that the diffraction peak is significantly more pronounced.

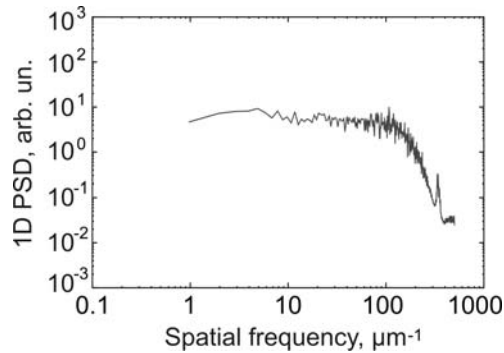


Figure 4: Average PSD of 6 TEM images that had been treated by the procedure discussed in the text.

6. Discussion and conclusion

The unexpected, on first glance, PSD results from the TEM images of the BPRML sample forced us to investigate the TEM images themselves. In this way, we discovered a strong asymmetry in probability distributions of the lower and higher levels of intensities of the TEM image of the BPRML test sample. The large variation in the high intensity values compared to the low intensity values could simply be a result of different instrumental responses to the different materials comprising the sample. Or it could be a result of data processing. In any case we have noticed strong evidence that the images are processed in some non-trivial way. Making a crude adjustment to correct for the disparity recovers a PSD much closer to the expected result.

While the TEM images of the BPRML sample appear to be of very high quality, from a metrological standpoint, PSD analysis of the TEM images actually indicates some limitations of the instrument. In the case of the low magnification TEM image, one can conclude that the spatial resolution is only about half as what would be expected based on the magnified pixel size.

The most probable cause of the metrological problems of TEM measurements is a contrast enhancement that is a usual practice of TEM image processing [7]. Indeed, a contrast of a direct TEM intensity measurement, e.g., obtained directly from the CCD detector, is often two low (<5-10%) in order to be recognized by a human eye. Therefore, in a TEM image the original contrast of a measured intensity distribution is processed to be enhanced for adaptation to the properties of human vision. Such image processing can be rather complicated and, of course, the result depends on the software used.

Acknowledgements

The Advanced Light Source is supported by the Director, Office of Science, Office of Basic Energy Sciences, Material Science Division, of the U.S. Department of Energy under Contract No. DE-AC02-05CH11231 at Lawrence Berkeley National Laboratory. Research at Brookhaven National Laboratory is sponsored by the U.S. Department of Energy under Contract No. DE-AC02-98CH10886.

References

- [1] V.V. Yashchuk, W.R. McKinney, P.Z. Takacs, Proc. SPIE 6704 (2007) 670408/1-12.
- [2] V.V. Yashchuk, W.R. McKinney, and P.Z. Takacs, Opt. Eng. 47(7) (2008) 073602/1-5.
- [3] S.K. Barber, P. Soldate, E.D. Anderson, R. Cambie, W.R. McKinney, P.Z. Takacs, D.L. Voronov, and V.V. Yashchuk, J. Vac. Sci. and Tech. B 27(6) (2009) 3213-9.
- [4] S.K. Barber, E.H. Anderson, R. Cambie, S. Marchesini, W.R. McKinney, P.Z. Takacs, D.L. Voronov, V.V. Yashchuk, Opt. Eng. 49(5) (2010) 053606/1-9.

- [5] S.K. Barber, E.D. Anderson, R. Cambie, W.R. McKinney, P.Z. Takacs, J.C. Stover, D.L. Voronov, V.V. Yashchuk, Nucl. Instr. and Meth. A 616(2-3) (2010) 172-182.
- [6] V.V. Yashchuk, E.H. Anderson, S.K. Barber, N. Bouet, R. Cambie, R. Conley, W.R. McKinney, P.Z. Takacs, D.L. Voronov, Proc. SPIE 7801 (2010) 7801-10/1-12.
- [7] E. E. Fenimore, T. M. Cannon, Appl. Opt. 17(3) (1978) 337-347.
- [8] D. B. Williams and C. Barry Carter, "Transmission Electron Microscopy. Part 3: Imaging," Second Ed. (Springer, New York, 2009).